Chemical Science

Cite this: *Chem. Sci.*, 2012, **3**, 2565

www.rsc.org/chemicalscience

EDGE ARTICLE

Prediction on the existence and chemical stability of cuprous fluoride

Aron Walsh,*[a] C. Richard A. Catlow,[b] Raimondas Galvelis,[b] David O. Scanlon,[b] Florian Schiffmann,[b] Alexey A. Sokol[b] and Scott M. Woodley[b]

Received 14th March 2012, Accepted 4th May 2012
DOI: 10.1039/c2sc20321a

The existence of CuF has been a matter of debate for the past century. A 1933 report of the synthesis of CuF in the sphalerite structure has never been reproduced, however, it consistently appears in textbooks and databases. We report the results from a computational study of CuF based on a hybrid density functional theory (DFT) approach and identify the cinnabar crystal structure as an energy minimum, which incorporates linear F–Cu–F chains that are characteristic of the Cu(I) ion. Assessment of the oxidation and disproportionation reactions reveals that while CuF is thermodynamically stable with respect to the standard state, it can be oxidised readily to form CuF_2. Moreover, *ab initio* molecular dynamics simulations reveal that the linear F–Cu–F chains have a low barrier to rotation, so that at moderate temperatures the material might not give rise to a clear diffraction pattern. The predicted ionization potential of 6.5 eV, with respect to the vacuum level, suggests that the material may be suitable for photochemical applications through the formation of a heterostructure with Cu_2O and/or ZnO.

Introduction

The unique properties of copper in the +1 oxidation state have been of longstanding interest in inorganic chemistry.[1] With a formal electronic configuration of $3d^{10}4s^0$, the ion is diamagnetic, but is readily oxidised to the +2 oxidation state, producing the open-shell, Jahn–Teller active, d^9 centre. Considering binary compounds, cuprous oxide, the cuprous chalcogenides and most cuprous halides are well-known and their physicochemical properties are fully characterised.[2]

The crystal structure of cuprous oxide is an interpenetrating network of linear O–Cu–O chains, which is considered to be stabilised primarily by the formation of a hybrid Cu d_{z^2}s orbital.[3] Mixing between s and d orbitals is symmetry forbidden in an octahedral or tetrahedral environment, but is allowed in a linear one. While the d^{10} electronic ground-state is non-degenerate, there are low lying d^9s^1 excited states that give rise to a second-order Jahn–Teller distortion analogous to s^2 lone pair systems.[4] For the chalcogenides, a more regular tetrahedral environment is generally adopted, which results in the wide variety of known Cu(I) containing multernary semiconductors based on the cubic sphalerite (zinc-blende) structure.[5] The cubic structure is also adopted by the cuprous halides, including CuCl, CuBr and CuI. Curiously, cuprous fluoride, CuF, was reported in the sphalerite structure in 1933,[6] however, there have been no recent reports of its synthesis, with the exception of a 1957 patent.[7] In addition to being the missing cuprous halide, CuF is also the absent member of the series of binary tetrahedral semiconductors formed from first row anions, *e.g.* SiC, GaN and ZnO.

In this work, we address the structure and thermodynamic stability of CuF using a combination of computational chemistry techniques. Through a series of first-principles calculations, we predict that CuF favours linear F–Cu–F chains that are satisfied in the chiral cinnabar structure. The material is stable with respect to its components, but unstable with respect to disproportion to form cupric fluoride, so that synthesis conditions and reaction kinetics should be carefully controlled to grow phase pure samples. However, the unique properties of the material provide motivation for its fabrication. In addition to the promise of non-linear optical response and conducting properties, the predicted ionisation potential of 6.5 eV bridges those of ZnO and Cu_2O, and a "type II" band offset is formed with both oxides, which could facilitate efficient conversion of long-wavelength visible light in photochemical or photovoltaic devices.

Methods

All calculations were performed at the level of Density Functional Theory (DFT),[8] with exchange–correlation effects treated using the PBEsol0 functional including 25% non-local Hartree–Fock exchange.[9] We utilized three computer codes for three different aspects of the work: cluster models, molecular dynamics simulations and accurate total energy calculations of the bulk phases. All computations were checked for convergence with

[a]*Centre for Sustainable Chemical Technologies and Department of Chemistry, University of Bath, Claverton Down, Bath BA2 7AY, UK. E-mail: a.walsh@bath.ac.uk*
[b]*University College London, Kathleen Lonsdale Materials Chemistry, Department of Chemistry, 20 Gordon Street, London WC1H 0AJ, UK*

respect to the basis sets, *k*-point sampling and quantum mechanical forces, each where appropriate.

The structure and total energy of CuF clusters were obtained using an all-electron DFT method with a local numerical orbital basis set, as implemented in the code FHI-AIMS.[10] A "Tier-2" basis was employed for each element, with scalar-relativistic effects treated at the ZORA level.[11] The details of the structure generation and optimization process have been discussed elsewhere.[12] The non-local exchange correlation terms were computed with an auxiliary basis (resolution of identity) formed by the products of the atomic basis functions.

The structure and total energy of the bulk phases of CuF were obtained using a plane-wave DFT method, as implemented in the code VASP.[13] The frozen-core electrons were treated within the projector augmented-wave method.[14] A plane-wave energy cut-off of 500 eV was used to define the basis set, with well-converged *k*-point sampling for each of the phases (a 6 × 6 × 2 Γ-point centred mesh was used for cinnabar). The Hartree–Fock component of the PBEsol0 functional was calculated using a soft augmentation charge. Note that the energies for all Cu(II) materials reported in Table 2 were based on spin-polarised calculations with the experimentally known ground-state magnetic ordering.

Finite-temperature dynamical simulations were performed within the code CP2K/Quickstep.[15] Here, the PBE0 functional[9b,16] was used due to the unavailability of the PBEsol0 functional, however, the minor change is not expected to affect any of the conclusions. The core electrons were modelled with Goedecker–Teter–Hutter *pseudo*potentials,[17] while the valence electronic density was represented by the hybrid Gaussian and plane wave basis sets scheme.[18] Short-range double-ζ valence basis set (DZVP-SR-MOLOPT[19]) with polarization functions (F) and without polarization functions (Cu), were combined with a plane wave density cut-off of 400 Ry. In order to reduce the computational cost of Hartree–Fock exchange, four approximations were employed: (i) integral and density matrix screening[20] (the Schwarz threshold was set to 1.0×10^{-5}); (ii) truncated Coulomb potential with long-range correction[21] (the truncation radius was set to 3.0 Å); (iii) auxiliary density matrix method[22] (the ADMM1 scheme, using an optimised basis set); (iv) Γ-point only, which is valid for the supercells considered. Details of the equilibration and production runs are reported in the results section.

Results and discussion

Ground-state crystal structure

The total energy of CuF in a range of binary crystal structures, including linear, tetrahedral and octahedral coordination environments, is reported in Table 1. For each case, the lattice vectors and internal positions were fully optimised. Remarkably, the lowest energy phase is found to be the hexagonal cinnabar structure, which is known for both HgO and HgS. The equilibrium structure (a = 3.29 Å, c = 9.16 Å) has two short Cu–F bonds (1.85 Å) with an angle between them of 179° and four long bonds at *ca*. 3 Å. As shown in Fig. 1(a), the structure consists of *pseudo*-1D CuF chains stacked along the hexagonal c axis.

Table 1 Calculated energy ranking of the bulk phases of CuF, relative to the cinnabar crystal structure

Phase (Strukturbericht notation)	Relative Energy (per CuF, eV)
Cinnabar (B9)	0.00
Graphite (A9)	0.15
NiAs (B8)	0.22
Sphalerite (B3)	0.23
Rocksalt (B1)	0.23
Wurtzite (B4)	0.24
1D cinnabar chain	0.21
0D $(CuF)_4$ nanocluster	0.17
1D $(CuF)_4$ stack	0.07
3D $(CuF)_4$ cubic crystal	0.05

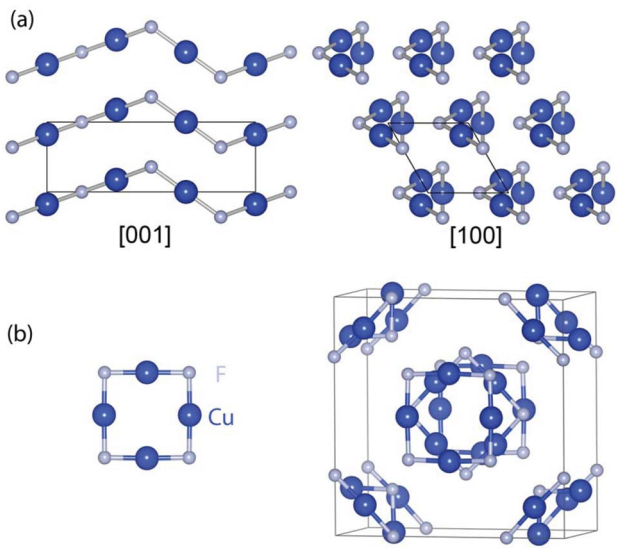

Fig. 1 (a) The predicted bulk crystal structure of CuF (space group 154, a = 3.29 Å, c = 9.16 Å); (b) the tetrameter building block of CuF nanoclusters and the corresponding cubic tetramer network.

Similar to the helical chains found in the chiral Sψ (more generally S∞) or *t*-Se crystal structures, the direction of rotation of the chains determines the stereochemical characteristics of the material. Left- or right-handed chains result in the two known enantiomers of cinnabar (D_3^4 or D_3^6). CuF may therefore exhibit optical dichroism and non-linear optical response, analogous to those observed for cinnabar and the elemental chalcogen (S, Se, Te) materials. The binding energy between 1D chains, as calculated by considering a single chain in a large supercell, was found to be 0.21 eV per CuF.

These results for the bulk material follow a recent investigation of the structural diversity of $(CuF)_{12}$ nanoclusters.[12] The global minimum configuration is found to consist of three $(CuF)_4$ tetrameric units that also preserve linear F–Cu–F bonds: a Cu square is inscribed in an F square rotated by 45°, as shown in Fig. 1 (b). Therefore, linear coordination is a motif that is favoured by both bulk and nanoscale CuF. We have found that the energy of the isolated $(CuF)_4$ tetramer is only 0.17 eV (per CuF) higher in energy than the cinnabar structure, while an infinite 1D stack of tetramers is just 0.07 eV higher. This tetramer is analogous to the X_8 molecular units forming a number of allotropes

of sulphur and selenium. A three-dimensional network constructed from the tetramer building block, shown in Fig. 1 (b), was found to be the second lowest energy structure.

Dynamic stability

While the cinnabar structure is locally stable at $T = 0$ K, we can also assess its dynamic stability at finite temperatures. To this end, we have performed an *ab initio* molecular dynamics study in the isothermal–isobaric ensemble with a flexible simulation cell and a time step of 0.5 fs. The temperature was maintained by the generalized Lengevin equation (GLE) thermostat[23] and the barostat time constant was set to 100 fs, with velocity rescaling performed every 10 fs.

The system was brought to thermal equilibrium at 300 K. While no changes were observed in the average Cu–F bond length within the *pseudo*-1D chain of cinnabar, the relative orientation of the chains were found to fluctuate so that the translational symmetry of the cinnabar crystal structure was broken. The behaviour is analogous to the elemental chalcogen solids, where a wide range of crystalline and amorphous allotropes have been observed, and as an inorganic equivalent of alkane polymers. Therefore, due to the small barrier to disorder, we anticipate that while the linear chains would be present in as-grown samples, a clear signature (such as a diffraction pattern) of the crystal structure may not be observable due to random rotations of the Cu–F chains. It is likely that the solid would exist in an amorphous state, with the local Cu–F bonding motif maintained.

Molecular dynamics simulations of the higher energy sphalerite phase demonstrated that it is dynamically stable at ambient temperatures, however, at very high temperatures (2700 K) it undergoes a spontaneous transformation to a layered structure with linear Cu–F bonds.

Thermodynamic stability

A physical reason for the absence of reports for CuF could be that the material is not thermodynamically stable. We have therefore investigated the fundamental chemical reactions involving the material, including the heats of formation, disproportionation and oxidation, as listed in Table 2. For the purpose of comparison, in addition to CuF, reaction energies are reported for the known compounds CuCl and Cu_2O.

First, we would like to comment on the controversial issue of the applicability of hybrid DFT approaches to systems with metallic behaviour, which is necessary for the calculation of the standard enthalpies of formation. Even though the screening of electrons described at the underlying Hartree–Fock level of theory is incorrect,[24] the recent application of these methods to the ground-state properties of normal metals have demonstrated their value in the calculation of thermodynamic cycles.[25] In this work, we have found that both the standard enthalpy of formation of gaseous Cu and known reaction enthalpies involving Cu(s) are reproduced to within 0.1 eV, while the equilibrium structural parameters within 1% of experiment.

The calculated formation enthalpies for all three materials are favourable and, in fact, CuF is the most exothermic at −2.29 eV (−221 kJ mol^{-1}). The calculated value for Cu_2O (−1.71 eV) compares well to the measured value of −1.75 eV.[26] However, all oxidation reactions are exothermic (at $T = 0$ K; gaseous partial pressure of 1 atm). The thermodynamic instability of Cu_2O at STP has been established,[27] however, the bulk material remains kinetically stable. The calculated heat of oxidation from cuprous to cupric oxide (−1.41 eV) again agrees well with the measured value of −1.51 eV,[26] which gives us confidence in our predictions for CuF. Moreover, the known structural and magnetoelectronic properties of the cupric materials are reproduced. It is worth noting that the Mott-insulator CuO has been a major challenge for materials modelling, where the standard local density or generalised gradient functionals, both pure and including a Hubbard U correction, fail dramatically.[2b,28]

The oxidation of CuF to CuF_2 is highly exothermic at −3.30 eV, so that any excess fluorine in the atmosphere will favour the formation of CuF_2. Finally, the disproportionation reaction considers the stability of the cuprous materials with respect to formation of the corresponding cupric compounds, and the precipitation of copper metal as a by-product. This reaction is only exothermic for CuF, therefore, the formation of some CuF_2 would be expected, especially at the material surface where ion mobility is enhanced. However, the growth of artificial heterostructures, for example using atomic layer deposition or molecular beam epitaxy, could provide a route to obtaining a phase pure material.

Table 2 Calculated thermodynamic stability of the cuprous halides and cuprous oxide. A reaction is endothermic where the enthalpy is positive. The enthalpy of formation for CuF, CuCl and Cu_2O are negative (exothermic reactions). The reaction of disproportionation for CuCl and Cu_2O is also endothermic, while that of CuF is exothermic. The reaction of oxidation is exothermic for all three materials

Chemical Reactions	Reaction Energy (eV)
Enthalpy of Formation	
$Cu(s) + \frac{1}{2}F_2(g) \rightarrow CuF(s)$	−2.29
$Cu(s) + \frac{1}{2}Cl_2(g) \rightarrow CuCl(s)$	−1.35
$2Cu(s) + \frac{1}{2}O_2(g) \rightarrow Cu_2O(s)$	−1.71
Enthalpy of Disproportionation	
$CuF(s) \rightarrow \frac{1}{2}CuF_2(s) + \frac{1}{2}Cu(s)$	−0.51
$CuCl(s) + \frac{1}{2}CuCl_2(s) + \frac{1}{2}Cu(s)$	0.62
$Cu_2O(s) \rightarrow CuO(s) \rightarrow Cu(s)$	0.15
Enthalpy of Oxidation	
$CuF(s) + \frac{1}{2}F_2(g) \rightarrow CuF_2(s)$	−3.30
$CuCl(s) + \frac{1}{2}Cl_2(g) \rightarrow CuCl_2(s)$	−0.11
$Cu_2O(s) + \frac{1}{2}O_2(g) \rightarrow 2CuO(s)$	−1.41

Electronic structure

The calculated electronic structure of CuF reveals two distinct low binding energy valence bands separated by a gap of 3 eV. As

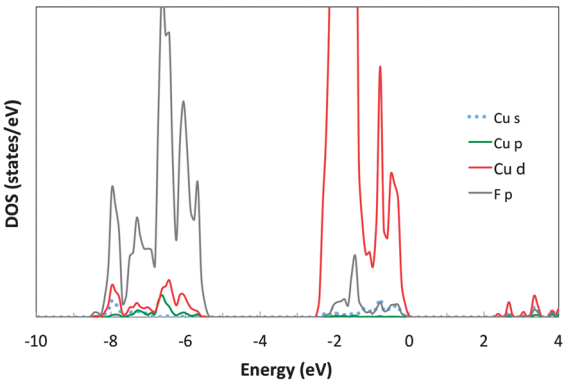

Fig. 2 Electronic density of states for CuF projected onto atomic spheres around each ion. The highest occupied state is set to 0 eV. The valence band consists of two main bands: (i) F p between −8 eV and −5.5 eV and (ii) Cu d between −2.5 eV and 0 eV.

shown in the electronic density of states, Fig. 2, the F 2p band is situated well below the upper Cu 3d valence band. This is in contrast to Cu(I) based oxides, where significant overlap between the cation d and anion p states is found.[29] From atomic calculations, the binding energy of the p orbital decreases from F (−12.51 eV) to O (−9.66 eV), Cl (−9.46eV) and S (−7.37 eV), while the Cu d and s orbital energies are −7.18 eV and −4.19 eV, respectively. Orbital interactions between F 2p and Cu 3d are expected to be marginal due to their large energy separation, while the differences for CuCl and Cu_2O are much smaller. This may be the underlying explanation for the competition between linear *versus* tetrahedral bonding, where lower coordination environments can be stabilised by the quadrupolar polarisation of Cu.

For CuF, the states at the top of the valence band are primarily Cu d_{xy} (orthogonal to the F–Cu–F bond), while the wavefunction at the bottom of the conduction band is a combination of Cu d_{z^2} and s orbitals, with an enhanced lobe in the *xy* plane that is shared between neighbouring Cu sites, as shown in Fig. 3. Considering the chemical nature of potential hole and electron carrier states described above, n- or p-type doped CuF has the strong possibility of exhibiting unusual and interesting behaviour.

CuF is predicted to be a wide band gap semiconductor or insulator. The calculated band gap is 3.0 eV and the valence band is situated 6.5 eV below the vacuum level, as determined from the (100) non-polar surface. The valence band position (ionisation potential) of Cu_2O thin-films has recently been measured at

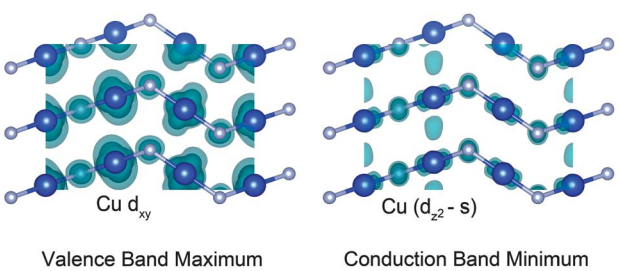

Fig. 3 Isosurface of the electron density associated with the band edge states in CuF.

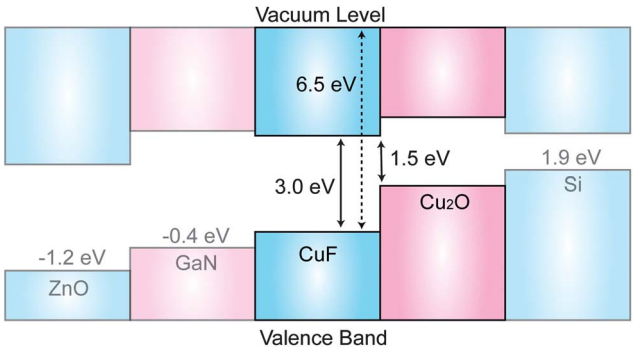

Fig. 4 Energy level alignment between CuF and Cu_2O. A "type II" offset of 1.5 eV should be formed at their interface, which could enable absorption of visible light and conversion into electron and hole carriers. The levels of other materials are shown for comparison and were taken from previous calculations (ZnO, GaN)[31] and experiment (Si).[26] The calculated alignment of ZnO and GaN with Cu_2O is in excellent agreement with the most recent XPS alignment experiments.[32]

approximately 5 eV below the vacuum level.[27] The calculation is therefore consistent with the expectation that due to the more electronegative anion, the valence band of CuF should be shifted to higher binding energy. The relative band alignment of CuF and Cu_2O with a range of other semiconducting materials is shown in Fig. 4. Remarkably, CuF fits naturally into this series of compounds, with a monotonic increase in work function from ZnO to CuF to Si.

One potential route for stabilising CuF is to form a heterostructure with a more robust oxide material, such as Cu_2O or ZnO. From the calculated band diagrams, either junction would result in a staggered "type II" band offset that could facilitate separation of electrons and holes and enable efficient visible light harvesting. The photoactivity of Cu_2O has been of recent interest for hydrogen production by water-splitting[30] and such an interface could help to extend the quantum efficiency to longer wavelengths than hitherto possible.

Conclusions

CuF is predicted to crystallise in the hexagonal cinnabar structure, however, the component 1D chains have a low barrier to rotation and may therefore give rise to an amorphous solid. The material is shown to be stable with respect to its components, but it is unstable with respect to CuF_2, which will require careful control of the growth conditions. However, the material is predicted to have the potential for a range of unique physical properties, including non-linear optics and semiconducting behaviour. Moreover, due to the high ionisation potential of CuF, we propose that a heterostructure formed with Cu_2O or ZnO could be beneficial for visible light harvesting in photochemical applications. Can contemporary synthetic chemistry meet this challenge?

Acknowledgements

The authors acknowledge support by an EPSRC Portfolio Partnership (Grant No. ED/D504872) and membership of the UK's HPC Materials Chemistry Consortium, which is funded by

EPSRC (Grant No. EP/F067496). Calculations were also performed on the University of Bath's High Performance Computing Facility. D. O. S. is grateful to the Ramsay Memorial Trust and University College London for the provision of a Ramsay Fellowship. A. W. acknowledges support from the Royal Society for a University Research Fellowship and the European Research Council for a Starting Grant.

References

1 F. A. Cotton, G. Wilkinson, C. A. Murillo and M. Bochmann, *Advanced Inorganic Chemistry*, Wiley, New York, 1999.
2 (*a*) A. Soon, X.-Y. Cui, B. Delley, S.-H. Wei and C. Stampfl, *Phys. Rev. B*, 2009, **79**, 035205; (*b*) M. Nolan and S. D. Elliott, *Phys. Chem. Chem. Phys.*, 2006, **8**, 5350; (*c*) W. M. Sears and E. Fortin, *Sol. Energy Mater.*, 1984, **10**, 93; (*d*) D. O. Scanlon, B. J. Morgan, G. W. Watson and A. Walsh, *Phys. Rev. Lett.*, 2009, **103**, 096405.
3 J. D. Dunitz and L. E. Orgel, *Adv. Inorg. Chem.*, 1960, **2**, 1.
4 A. Walsh, D. J. Payne, R. G. Egdell and G. W. Watson, *Chem. Soc. Rev.*, 2011, **40**, 4455.
5 S. Chen, X. G. Gong, A. Walsh and S.-H. Wei, *Phys. Rev. B*, 2009, **79**, 165211.
6 F. Ebert, H. Woitinek and Z. Anorg, *Z. Anorg. Allg. Chem.*, 1933, **210**, 269.
7 D. A. Mccauly, Office, U.S. P., Ed. USA, 1957, vol. 2817576.
8 (*a*) W. Kohn and L. J. Sham, *Phys. Rev.*, 1965, **140**, A1133; (*b*) P. Hohenberg and W. Kohn, *Phys. Rev.*, 1964, **136**, B864.
9 (*a*) J. P. Perdew, A. Ruzsinszky, G. I. Csonka, O. A. Vydrov, G. E. Scuseria, L. A. Constantin, X. Zhou and K. Burke, *Phys. Rev. Lett.*, 2008, **100**, 136406; (*b*) M. Marsman, J. Paier, A. Stroppa, G. Kresse and J. Phys., *J. Phys.: Condens. Matter*, 2008, **20**, 064201; (*c*) F. Corà; M Alfredsson; G. Mallia; D. S. Middlemiss; W. C. Mackrodt; R. Dovesi; R. Orlando; Springer: Berlin, 2004.
10 (*a*) V. Havu, V. Blum, P. Havu and M. Scheffler, *J. Comput. Phys.*, 2009, **228**, 8367; (*b*) V. Blum, R. Gehrke, F. Hanke, P. Havu, V. Havu, X. Ren, K. Reuter and M. Scheffler, *Comput. Phys. Commun.*, 2009, **180**, 2175.
11 E. Vanlenthe, E. J. Baerends and J. G. Snijders, *J. Chem. Phys.*, 1994, **101**, 9783.
12 A. A. Sokol, C. R. A. Catlow, M. Miskufova, S. A. Shevlin, A. A. Al-Sunaidi, A. Walsh and S. M. Woodley, *Phys. Chem. Chem. Phys.*, 2010, **12**, 8438.
13 (*a*) G. Kresse and J. Furthmüller, *Phys. Rev. B*, 1996, **54**, 11169; (*b*) G. Kresse and J. Furthmüller, *Comput. Mater. Sci.*, 1996, **6**, 15.
14 P. E. Blöchl, *Phys. Rev. B*, 1994, **50**, 17953.
15 J. Vandevondele, M. Krack, F. Mohamed, M. Parrinello, T. Chassaing and J. Hutter, *Comput. Phys. Commun.*, 2005, **167**, 103.
16 J. P. Perdew, K. Burke and M. Ernzerhof, *Phys. Rev. Lett.*, 1996, **77**, 3865.
17 S. Goedecker, M. Teter and J. Hutter, *Phys. Rev. B*, 1996, **54**, 1703.
18 G. Lippert, J. Hutter and M. Parrinello, *Mol. Phys.*, 1997, **92**, 477.
19 J. Vandevondele, *J. Chem. Phys.*, 2007, **127**, 114105.
20 M. Guidon, F. Schiffmann, J. Hutter and J. Vandevondele, *J. Chem. Phys.*, 2008, **128**, 214104.
21 M. Guidon, J. Hutter and J. Vandevondele, *J. Chem. Theory Comput.*, 2009, **5**, 3010.
22 M. Guidon, J. Hutter and J. Vandevondele, *J. Chem. Theory Comput.*, 2010, **6**, 2348.
23 M. Ceriotti, G. Bussi and M. Parrinello, *Phys. Rev. Lett.*, 2009, **103**, 030603.
24 N. W. Ashcroft and N. D. Mermin, *Solid State Physics*, Brooks/Cole, Belmont, 1976.
25 (*a*) J. Paier, M. Marsman, K. Hummer, G. Kresse, I. C. Gerber and J. G. Angyan, *J. Chem. Phys.*, 2006, **124**, 154709; (*b*) J. Paier, M. Marsman and G. Kresse, *J. Chem. Phys.*, 2007, **127**, 024103.
26 D. R. Lide, *CRC Handbook of Chemistry and Physics*, CRC Press, Boca Raton, FL, 2007.
27 J. Deuermeier, J. Gassmann, J. Brotz and A. Klein, *J. Appl. Phys.*, 2011, **109**, 113704.
28 D. O. Scanlon, B. J. Morgan and G. W. Watson, *J. Chem. Phys.*, 2009, **131**, 124703.
29 (*a*) D. O. Scanlon, A. Walsh, B. J. Morgan, G. W. Watson, D. J. Payne and R. G. Egdell, *Phys. Rev. B*, 2009, **79**, 035101; (*b*) T. Arnold, D. J. Payne, A. Bourlange, J. P. Hu, R. G. Egdell, L. F. J. Piper, L. Colakerol, A. De Masi, P.-A. Glans, T. Learmonth, K. E. Smith, J. Guo, D. O. Scanlon, A. Walsh, B. J. Morgan and G. W. Watson, *Phys. Rev. B*, 2009, **79**, 075102.
30 A. Paracchino, V. Laporte, K. Sivula, M. Gratzel and E. Thimsen, *Nat. Mater.*, 2011, **10**, 456.
31 A. Walsh, C. R. A. Catlow, M. Miskufova and A. A. Sokol, *J. Phys.: Condens. Matter*, 2011, **23**, 334217.
32 B. Kramm, A. Laufer, D. Reppin, A. Kronenberger, P. Hering, A. Polity and B. K. Meyer, *Appl. Phys. Lett.*, 2012, **100**, 094102.